

Flux Weakening Operation of Switched Reluctance Motors

T. Humiston, Student Member, IEEE
Department of Electrical and Computer Engineering
Clarkson University
Potsdam, NY 13699

P. Pillay, Senior Member, IEEE
Department of Electrical and Computer Engineering
Clarkson University
Potsdam, NY 13699

Abstract: Speed can be increased above base speed by flux weakening in the DC machine. The relationships of torque, power and speed have been characterized for the DC machine when operating from zero speed to twice base speed. To date, no such research has been performed on the Switched Reluctance Motor (SRM) above base speed. This paper focuses on characterizing the relationships of torque, power and speed during high speed operation of the SRM. In doing so it is necessary to examine the Back-EMF as speed increases from zero speed up to and including twice base speed.

A complete set of dynamic curves are developed including flux-linkage, current, torque, back-emf and instantaneous power, over the entire speed range from zero to twice base. In addition, the characterization curves for rms phase current, average DC link current, phase voltage, machine losses, torque, input power and developed power are also presented.

I. INTRODUCTION

The first switched reluctance motor (SRM) dates back to the nineteenth century [1, 2]. Development of the SRM was slowed by the unavailability of fast switching devices. Very little progress was made until the 1960's and the development of the thyristor [3]. Since then several advancements have been made in recent years among them being advances in power electronics and modeling of the SRM. This has spawned a renewed interest in the SRM which is continuing to grow as additional developments are made. With improving modeling techniques for both machine and drive along with CAD, the SRM is becoming a serious competitor with AC and DC machines.

The SRM has competitive power density, starting torque, torque to inertia ratio, fault tolerance, speed range, efficiency, manufacturing costs, material costs and reliability [1, 4] when compared to conventional machines. This is a result of its double salient pole design. Its simple construction lends itself to lower manufacturing costs. The rotor is a simple laminated design with no windings or magnets. As a result extremely high speeds can be obtained when compared to rotors with magnets or windings. The simplicity of the stator is another advantage. The windings are much simpler than those for induction machines, with the capability of manufacturing the coils separately and installed subsequently into the machine. This also lowers maintenance costs if a winding needs to be changed. Other advantages include a high starting torque which can be achieved without large inrush currents and that the torque is independent of current direction. High efficiency is maintained over a wide range of speed.

The switched reluctance motor has disadvantages in acoustic noise and torque ripple, the magnitude of which changes with the number of phases. This ripple is also

responsible for part of the motor's noise problem. Another source for noise in the SRM is the ovalizing that occurs in the stator from opposite poles attracting and pulling towards each other during excitation and returning to their natural position when unexcited. The need for a minimal air gap is another disadvantage of the SRM in that it requires higher manufacturing tolerances. There are disadvantages associated with the control of the SRM. For example, rotor position is needed for excitation control. Also only one motor can be operated per inverter. Since each phase of the SRM has a pair of coil leads to be connected, the cabling for the motor is more complex than other machine types. The advantages outweigh the disadvantages in many applications, resulting in a wide number of applications.

The relationships of torque, power and speed in the SRM have been investigated and characterized up to base speed. However, above base speed the characterization of these relationships are yet undetermined or at least no formal work has been presented in this area. This paper focuses on this operating region, of the SRM, to establish these relationships. To proceed with the investigation it is first necessary to review the torque, power and speed relationships in the DC machine as it is felt that this will provide a good base from which to develop the theory for the SRM.

In addition to the torque, power and speed characteristics, the back-emf in the SRM is investigated both at base and above base speed. To date very little has been published regarding the back-emf in the SRM.

II. FLUX WEAKENING OPERATION IN THE DC MACHINE

During the operation of the DC machine, whether it is below, at or above base speed, it is important that the rated values of voltage and current not be exceeded or damage to the machine will occur. The torque, power and speed curves discussed in this section represent the envelope of operation for the DC machine. The armature current (I_a) is held constant at its rated value during the development of these curves to yield the maximum torque. The curves are divided into two regions as follows: The first region from zero speed up to and including base speed, known as the constant torque region. The second region is above base speed, typically up to twice base speed, known as the constant power region.

The operational characteristics of the DC machine are represented by several equations as follows:

$$V_a = B_{emf} + (I_a * R_a) \quad (2.1)$$

where B_{emf} is the back-emf.

$$B_{emf} = K_t * \phi * \omega \quad (2.2)$$

where,

$$\phi = K_\phi * I_f \quad (2.3)$$

and substituting in (2.2), yields

$$Bemf = K_t * K_\phi * I_f * \omega \quad (2.4)$$

$$P_{in} = V_a * I_a \quad (2.5)$$

$$P_{developed} = P_{in} - \text{losses} \quad (2.6)$$

where the losses associated with the armature are equal to

$$\text{Losses} = I_a^2 * R_a \quad (2.7)$$

Substituting (2.5), and (2.7), into (2.6), yields

$$P_{developed} = V_a * I_a - I_a^2 * R_a \quad (2.8)$$

Rearranging

$$P_{developed} = I_a * (V_a - I_a * R_a) \quad (2.9)$$

Equation (2.1) can be rearranged to yield

$$Bemf = V_a - I_a * R_a \quad (2.10)$$

which can then be substituted into (2.9), giving

$$P_{developed} = I_a * Bemf \quad (2.11)$$

Equations for developed torque are:

$$\tau_{developed} = \frac{P_{developed}}{\omega} \quad (2.12)$$

and substituting (2.11), gives

$$\tau_{developed} = \frac{I_a * Bemf}{\omega} \quad (2.13)$$

and if (2.2) is substituted into (2.13),

$$\tau_{developed} = K_t * \phi * I_a \quad (2.14)$$

To construct the curves for the constant torque region we know, that I_a , I_f and $\tau_{developed}$ are constant so the only way for speed to vary in this region is, from (2.4), for the back-emf to vary. Hence, from (2.1), the armature voltage must vary from zero volts at zero speed to rated voltage at base speed. Next, to construct the curves for the constant power region, with V_a , I_a , $Bemf$ and $P_{developed}$ all constant, the only way for speed to increase is (from (2.4)) for I_f to decrease. When I_f decreases, the flux produced in the machine decreases (equation (2.3)).

The results from both regions are combined to form a complete set of curves characterizing the full range of operation from zero speed through to twice base speed. Fig. 1, shows the complete torque and power verses speed curves, and Fig. 2, the armature voltage and back-emf verses speed curves.

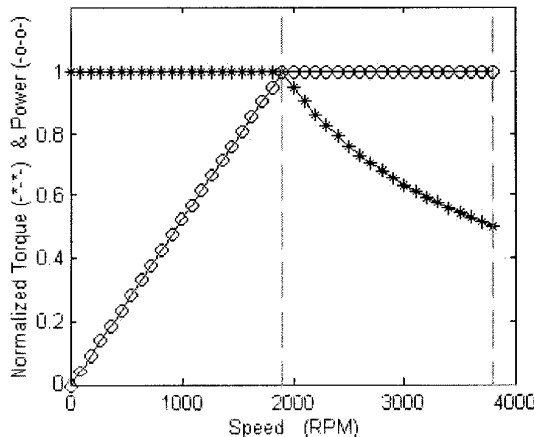


Fig. 1. Torque and power vs. speed

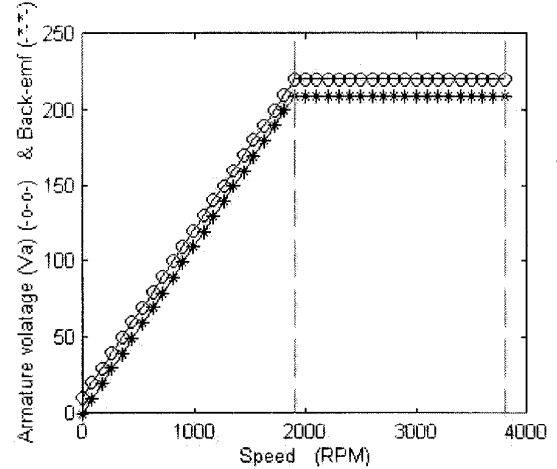


Fig. 2. Armature voltage and back-emf vs. speed.

With an understanding of the relationships of torque, power and speed as well as the importance of back-emf in the DC machine, the relationships in the SRM are now examined.

III. DEVELOPING THE THEORY FOR THE SRM.

In the SRM, like in the DC machine, the machines rated values are not to be exceeded. This should lead to two separate regions of operation similar to that of the DC machine, a constant torque region up to and including rated speed and a constant power region above base speed up to twice base speed. With the DC machine, the armature current is held constant over the entire range of operation. For the SRM, the rms value of the current in each phase is held constant since this determines the conduction losses.

The constant torque region is discussed first, where in the SRM it is the constant average torque that is being considered. The phase torque waveforms are summed then averaged over one complete revolution to yield the average value. As torque is a function of coenergy and angular position to keep torque constant both coenergy and angular position have to be held constant over this region. Coenergy is a function of flux-linkage and current and since current is already being held constant, flux-linkage has to be held constant. Note that flux is also constant in the DC machine during constant torque operation. Using the equation for flux-linkage.

$$\Psi(t) = \int_0^t (V(t) - R I(t)) dt \quad (3.1)$$

and making a substitution of

$$dt = d\theta / \omega \quad (3.2)$$

yields

$$\Psi(\theta) = \int_0^\theta \left(\frac{V(\theta) - I(\theta) * R}{\omega} \right) d\theta \quad (3.3)$$

To hold the second constraint on torque, angular position, constant and to maintain a constant current, the firing and excitation angles will be held constant maintaining a constant

conduction period as well. With angular position θ held constant (3.3) reduces to

$$\Psi = \frac{V - I \cdot R}{\omega} \quad (3.4)$$

With I constant, R is constant and ω increasing linearly from zero to base speed the only way for flux-linkage to remain constant is for V to increase in proportion to ω . This is how speed is changed in the DC machine in the constant torque region. The SRM will be operated under these conditions where only the supply voltage will be adjusted to vary speed during the constant torque region.

In the constant power region the rms phase current is held constant in addition to the DC bus voltage, as for the DC machine. Referring to (3.4) with I , R and V constant, the only way speed (ω) can increase is for flux-linkage (Ψ) to decrease. So, like the DC machine, the constant power region in the SRM will be a region of flux weakening. The difference being that in the DC machine the flux was weakened by reducing the field current but the SRM does not have a separate field. To weaken the flux-linkage in the SRM, the excitation period will be adjusted advancing the firing and extinguishing angles. Both adjustments occur at the same time with the firing angle advanced more than the extinguishing angle, i.e. approximately 11.5 degrees for the firing angle versus 4.8 degrees for the extinguishing angle.

It should be noted that since the rms values of the current are being used and that current is dependant on the conduction period as well as the angles used, there are an infinite number of combinations of firing and extinguishing angles possible at each speed that will yield the same rms value. However, only one combination can produce the maximum average torque at each speed. It is this combination that is used for the characterization of torque, power and speed curves. This combination is determined through several iterations of machine equations until the solution is found. Several possibilities were eliminated by a simple set of rules governing the firing and extinguishing angles. The firing angle has to be on or before the unaligned position. For obvious reasons extinguishing angle cannot be before the firing angle. The extinguishing angle also cannot be after the aligned position as large amounts of negative torque will be developed, reducing the overall output and efficiency. With these constraints the optimal solution is easily attained.

It is instructive to examine back-emf in the SRM. In the DC machine the back-emf is not allowed to exceed the armature voltage minus the product of armature current and resistance. This is another place where the two machine types differ, from the equation for the SRM,

$$V_\phi = L_\phi \cdot \frac{di}{dt} + \text{Bemf} \quad (3.5)$$

if $L \cdot \frac{di}{dt}$ is a positive value then back-emf has to be less than

V_ϕ , but a negative $L \cdot \frac{di}{dt}$ indicates that the back-emf can be larger than V_ϕ . From the equation,

$$\text{Bemf} = \omega \cdot \frac{\partial \Psi}{\partial \theta} \quad (3.6)$$

back-emf is dependant on speed and flux-linkage. From (3.5), when V_a is constant, the current waveform is dependant in part on the back-emf. With this in mind when the back-emf is less than the phase voltage the current will increase, a positive $\frac{di}{dt}$. At the point where the back-emf equals the

phase voltage the corresponding $\frac{di}{dt}$ is zero momentarily, and

then goes negative once the back-emf exceeds the phase voltage causing the current to decrease. Current will continue to decrease as long as the back-emf is larger than the phase voltage. The slope of the current decay is greater, the larger the magnitude of the back-emf relative to the DC bus. The back-emf thus affects the torque waveshape thus affecting the average torque developed. With this difference in back-emf in the SRM, especially above base speed, the torque, power and speed characteristics above base speed may not follow the same trend as with the DC machine.

IV. WAVEFORM AND ENVELOPE RESULTS FOR THE SRM

The results have been divided into two sections one covering the dynamic results of operation over the range of speeds, the other covering the characteristic curves of the SRM over the full range of operation through twice base speed. The following table shows the conduction angles, phase current and phase voltage used for the various speed increments.

Table 4.1 Results of PC-SRD iterations

speed	Firing angle	Extn. Angle	I rms	Torque	Vdc
250	28.2	51.9	9.43	24.29	50.5
500	28.2	51.9	9.43	24.43	91.9
750	28.2	51.9	9.43	24.42	133.4
1000	28.2	51.9	9.43	24.37	174.9
1250	28.2	51.9	9.43	24.35	216.5
1500	28.2	51.9	9.43	24.29	258
1750	25.9	51.6	9.44	22.09	258
2000	23.8	50.9	9.43	20.07	258
2250	21.9	50.5	9.44	18.38	258
2500	20.1	49.7	9.43	16.96	258
2750	18.4	48.8	9.42	15.65	258
3000	16.7	47.1	9.43	14.325	258

Section one: The dynamic results.

Fig. 4, shows the complete set of flux-linkage curves ranging from 250 rpm to 3000 rpm in increments of 250 rpm. During the constant torque region (0-1500 rpm) flux-linkage remains constant. There is a slight change in the curves after excitation is past but this amounts to only 1/2 percent change in the average flux-linkage. Once base speed (1500 rpm) is past the flux-linkage weakens, as speed increases through the high speed region. The highest curve shown in Fig. 4, is for 1500 rpm and the lowest for 3000 rpm. The average flux-linkage value decreases by 35 percent at twice base speed which is quite different from the 50 percent decrease seen in the DC machine. This brings into question if this region is constant power.

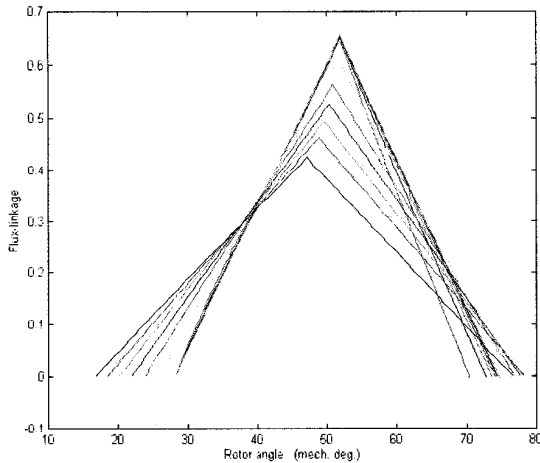


Fig. 4. Complete set of flux-linkage curves for one period of one phase, from 250 to 3000 rpm.

Fig. 5, shows the complete set of current curves ranging from 250 rpm to 3000 rpm. For all the curves the rms value remains the same. During the constant torque region the firing and extinguishing angles remain the same over the speed range from zero to base. There is only a slight difference in the curves in this region with no significant change in the rms value of the current.

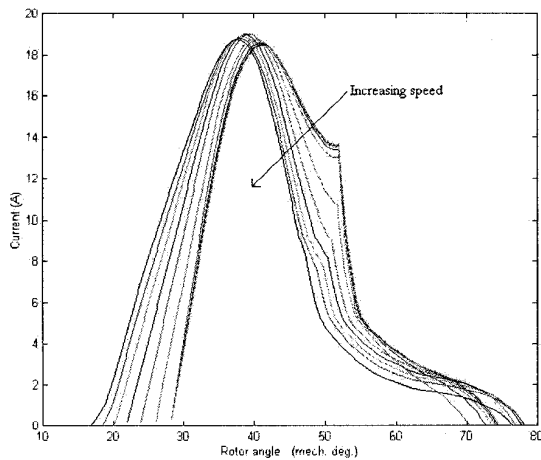


Fig. 5. Complete set of current curves for one period of one phase, from 250 to 3000 rpm.

This difference is associated with the 1/2 percent change in the flux-linkage within this region. In the high speed region the firing and extinguishing angles are varied by the values in table 4.1. This causes the curves to shift to the left, advancing with rotor position. Referring to Fig. 5, the curve farthest to the right is for 1500 rpm while the curve farthest to the left is for 3000 rpm.

Fig. 6, shows the complete set of torque curves ranging from 250 rpm to 3000 rpm. In the region from zero speed up to base speed all the curves are the same verifying that this is a region of constant torque. In the high speed region the

torque decreases as speed increases. The highest curve is at 1500 rpm and the lowest curve is at 3000 rpm.

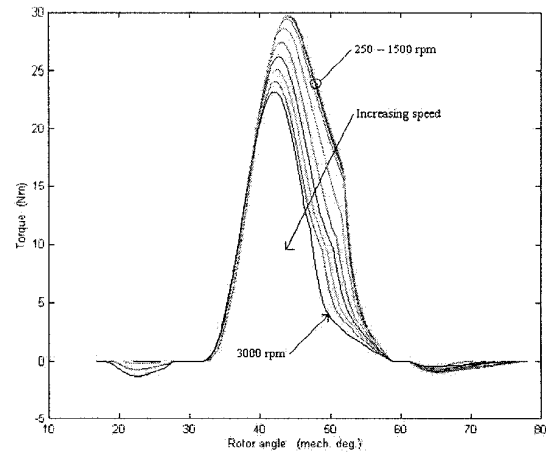


Fig. 6. Complete set of torque curves for one period of one phase, from 250 to 3000 rpm.

The complete set of back-emf curves are shown in Fig. 7, ranging from 250 rpm to 3000 rpm. In the constant torque region the back-emf increases as speed increases. The lowest curve is at 250 rpm. This increasing trend continues in the high speed region, where the highest curve is at 3000 rpm. The rms value of back-emf also increases over the entire range of speeds.

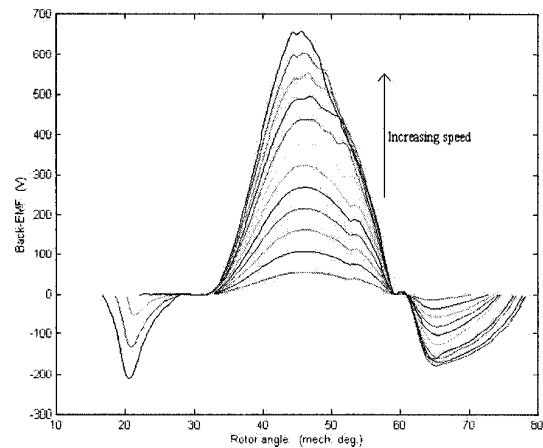


Fig. 7. Complete set of back-emf curves for one period of one phase, from 250 to 3000 rpm.

Fig. 8, shows the complete set of instantaneous power curves ranging from 250 rpm (lowest curve) to 3000 rpm (highest curve). In the constant torque region the instantaneous power increases with speed. However, in the region from base speed to twice base speed the curves are not constant power. Instantaneous power continues to increase with speed but at a lower rate than during the constant torque region. This change in the trend will be discussed further, below.

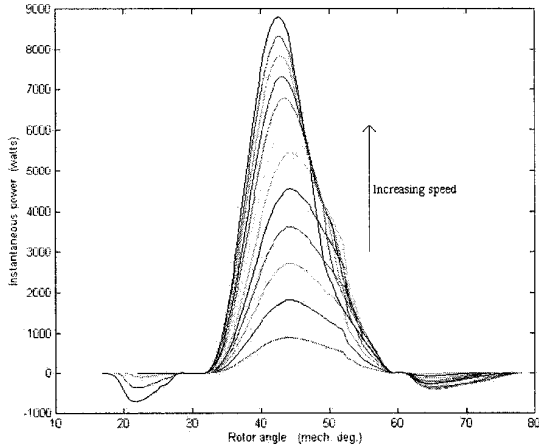


Fig. 8. Complete set of instantaneous power curves for one period of one phase, from 250 to 3000 rpm.

Section Two: The characteristic curves.

The curves below represent the operational characteristics of the Oulton 8/6 SRM from 250 rpm through 3000 rpm with particular attention focused on the region from 1500 rpm (base) to 3000 rpm. The characteristics of the rms phase current and average DC link current are shown in Fig. 9, the rms phase current remains constant over the operating range as intended.

The average DC link current does not remain constant however. In the constant torque region the average DC link current decreases as base speed is approached. This comes about since input power has to track output power by the difference of machine losses. Input power is the product of instantaneous phase voltage and instantaneous DC link current.

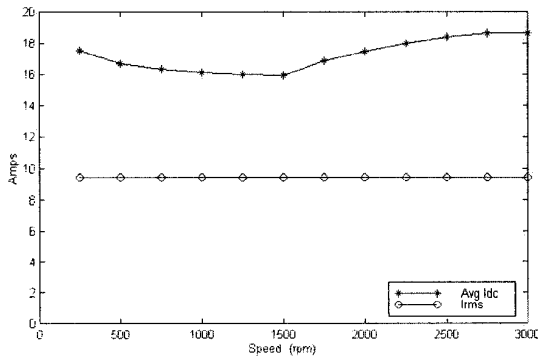


Fig. 9. Rms phase current and average DC link current.

Fig. 10, shows that the phase voltage curve has a slightly different slope than the input power curve. This difference in slope affects the DC link current. As the change in slope of the voltage becomes less at lower speeds the current increases to maintain the constant slope of the input power curve. Once base speed has been reached, the phase voltage becomes constant, the slope of the DC link current curve matches the slope of the input power curve.

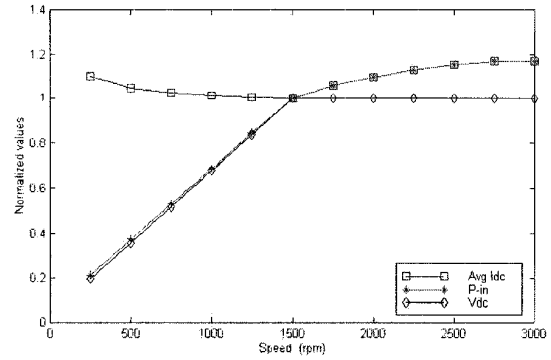


Fig. 10. Phase voltage, input power and average DC link current.

Fig. 11 shows the phase voltage over the full range of operation. In the region of flux weakening in the DC machine the field current is decreased while armature current remained constant. Here we see that during flux weakening in the SRM, the average DC link current increases while rms phase current remains constant as shown in Fig. 9.

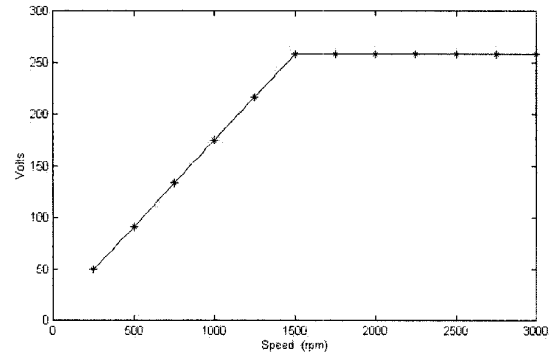


Fig. 11. Plot of phase voltage over complete operating range.

The losses associated with the machine are shown in Fig. 12. Since coil resistance remains constant, once the machine has reached thermal steady state, and since the rms phase current is held constant, the $I^2 \cdot R$ loss remains constant over the entire range. The Iron loss changes with speed. In the region up to base speed the iron loss increases in proportion but above base speed, the loss becomes almost constant.

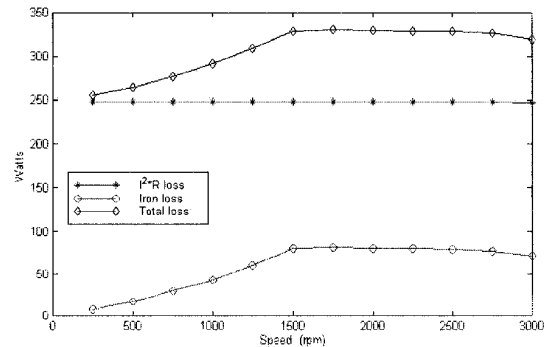


Fig. 12. Plot showing the machine losses over entire operating range.

This occurs since the flux in the iron is decreased in order for speed to increase causing the net loss to remain constant.

The torque, power and speed curves are shown Fig. 13. The region from zero speed to base speed is the constant torque region with power increasing linearly as speed increases. The region from base speed up to twice base speed is not a constant power region as in the DC drive case. Because flux-linkage decreased by only 35 percent, unlike the 50 percent decrease in the DC machine, the torque does not decrease as much as for the DC machine. The torque decrease is only 41 percent. Unlike the DC machine where power has to remain constant not to exceed machine voltage and current ratings, in the SRM the power can increase. While the power has increased the machine's rated values have not been exceeded as the DC link voltage remains constant as did the rms current. The reason for this difference between the SRM and the DC machine is that the rms current can be kept constant but because of the change in the waveform, the average current can increase, resulting in greater output power. Of course the output power increase can only occur with a corresponding increase in the input power, but this is done without exceeding the machine's ratings.

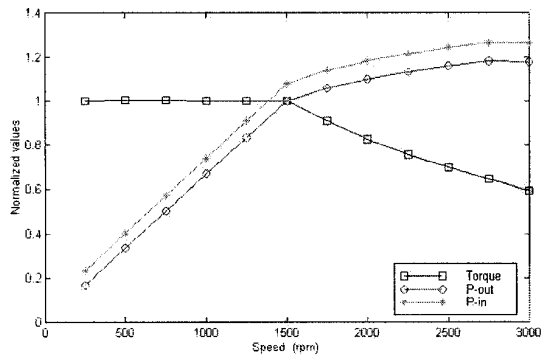


Fig. 13. Plot showing torque, power and speed characteristics over entire speed range.

V. CONCLUSIONS

A review of torque, power and speed characteristics in the DC machine was presented as an aid in developing the theory for determining these characteristics in the SRM. A set of guidelines was developed towards determining the torque, power and speed characteristics. The back-emf was studied in detail. The static and dynamic characteristics of the SRM when operating above and below base speed were determined and presented.

The SRM has a constant torque region up to base speed. However, above base speed it was found that power can continue to increase, while staying within the machine's ratings. Coinciding with this increase in power is a decrease in the developed torque that is lower than that of a DC machine. This is an advantage of the SRM over the DC machine.

VI. REFERENCES:

- [1] T. J. E. Miller, "Switched Reluctance Motors and Their Control", *Magna Physics Publishing*, 1993.
- [2] M. Moallem and C. M. Ong, "Predicting the Steady-State Performance of a Switched Reluctance Machine", *IEEE Transactions on Industry Applications*, Vol. 27, No. 6, November/December 1991, pp. 1087-1097
- [3] W. F. Ray, P. J. Lawrenson, R. M. Davis, J. M. Stephenson, N. N. Fulton, and R. J. Blake, "High-Performance Switched Reluctance Brushless Drives", *IEEE Transactions on Industry Applications*, Vol. IA-22, No. 4, July/August 1986, pp.722-730
- [4] Y. Tang, "Characterization, Numerical Analysis, and Design of Switched Reluctance Motors", *IEEE Transactions on Industry Applications*, Vol. 33, No. 6, November/December 1997, pp. 1544-1

VII. BIOGRAPHIES

Timothy J. Humiston (S'97) received the Bachelor of Science degree in Electrical Engineering in 1998 and the Master of Science degree in Electrical Engineering in 2000 from Clarkson University, Potsdam, NY. He is currently working towards the Ph.D. degree in Electrical Engineering at Clarkson University, Potsdam, NY.

He is a student member of the IEEE and a member of the Power Engineering, Industrial Applications, and Power Electronics Societies. His research interests are in machines and drives relating to the switched reluctance and induction machines. He also has an interest in machines and drives applications for electric vehicles. His current work is in surge propagation in the windings of the induction machine.

Dr Pragasen Pillay (S'84-M'87-SM'92) received the Bachelor's degree from the University of Durban-Westville in South Africa in 1981, the Master's degree from the University of Natal in South Africa in 1983 and the Ph.D from Virginia Polytechnic Institute & State University in 1987, while funded by a Fulbright Scholarship.

From January 1988 to August 1990 he was with the University of Newcastle upon Tyne in England. From August 1990 to August 1995 he was with the University of New Orleans. Currently he is with Clarkson University, Potsdam, NY 13699, where he is a Professor in the Department of Electrical & Computer Engineering and holds the Jean Newell Distinguished Professorship in Engineering. He is a Senior Member of the IEEE and a member of the Power Engineering, Industry Applications, Industrial Electronics and Power Electronics Societies. He is a member of the Electric Machines Committee, Chairman of the Industrial Drives within the Industry Applications Society and Vice-Chairman of Induction Machinery Sub-Committee in the Power Engineering Society. He is a member of the IEE, England and a Chartered Electrical Engineer. He has organized and taught short courses in electric drives at the Annual Meeting of the Industry Applications Society. His research and teaching interests are in modeling, design and control of electric motors and drives for industrial and alternate energy applications.